JOURNAL OF AGRICULTURAL AND FOOD CHEMISTRY
ARTICLE

J. Agric. Food Chem. XXXX, XXX, 000–000 A
DOI:10.1021/jf904249f

Comparison of FTIR Spectra between Huanglongbing (Citrus Greening) and Other Citrus Maladies

Samantha A. Hawkins,*,† Bosoon Park,† Gavin H. Poole,‡ Tim R. Gottwald,‡ William R. Windham,† Joseph Albano,‡ and Kurt C. Lawrence†

†Russell Research Center, Agricultural Research Service, U.S. Department of Agriculture, 950 College Station Road, Athens, Georgia 30605, and ‡U.S. Horticultural Research Laboratory, Agricultural Research Service, U.S. Department of Agriculture, Fort Pierce, Florida 34945

Fourier transform infrared (FTIR) spectroscopy has the ability to quickly identify the presence of specific carbohydrates in plant materials. The presence of the disease huanglongbing (HLB) in the leaves of infected citrus plants has a distinctive spectrum that can be used to distinguish an infected plant from a healthy plant. However, many citrus diseases display similar visible symptoms and are of concern to citrus growers. In this study several citrus diseases (citrus leaf rugose virus, citrus tristeza virus, citrus psorosis virus, and *Xanthomonas axonopodis*) and nutrient deficiencies (iron, copper, zinc, manganese, and magnesium) were compared with HLB using FTIR spectroscopy to determine if the spectra alone can be used to identify plants that are infected with HLB instead of another disease. The results indicate that the spectra of some diseases and deficiencies more closely resemble those of apparently healthy plants and some share the carbohydrate transformation that has been seen in the spectra of HLB-infected plants.

KEYWORDS: Citrus greening; HLB; huanglongbing; FTIR spectroscopy; chemometrics

INTRODUCTION

Myriad diseases that affect citrus plants have been detected in the United States (*1*−*5*). Citrus disease effects can range from rendering a season's crop useless to having to eradicate an entire orchard (*1*,*4*−*9*). Some common pathogens affecting citrus plants include citrus leaf rugose virus (CLRV), which causes leaf rugose, citrus tristeza virus (CTV), which causes citrus decline and stem pitting, citrus psorosis virus (CPsV), which causes psorosis and back scaling, and *Xanthomonas axonopodis*, which causes citrus canker (*1*−*3*,*10*,*11*). Some common nutrient deficiencies of citrus that are of concern include iron, copper, zinc, manganese, and magnesium deficiencies (*10*, *11*). One other disease that has recently emerged in the United States is citrus greening disease, also known as huanglongbing (HLB) (*4*−*6*,*8*,*9*,*12*,*13*). HLB falls into the category of orchard-destroying diseases. The symptoms appearing on the leaves of many of these infected trees are similar and include small leaves, chlorosis, blotchy mottling, and various levels of discoloration. In the case of HLB, the fruit becomes small, misshapen, discolored with green areas, and bitter. Eventually the HLB-infected tree stops producing fruit altogether. Some of the other diseases or nutrient deficiencies can affect the quality of the fruit, but they generally do not decimate the orchard as completely as HLB can.

HLB disease was first detected in Florida in 2005 (*6*). As of October 2009, it has been confirmed in 34 counties in Florida (*14*). Additionally, its presence has been confirmed in June 2008 in Louisiana and in April 2009 in Charleston County, South Carolina (*4*, *15*). HLB is associated with a bacteria, *Candidatus* Liberibacter sp., which is carried by a psyllid vector (*8*). The psyllid vectors carrying the bacteria associated with HLB have also been detected in California, Texas, Mississippi, Alabama, and Georgia (*15*). The potential for destruction of the citrus industry is great if the spread of the disease is not curbed.

Current methods in use for detection of diseases in citrus plants include classification by visual inspection by trained personnel in the groves, classification by microbiologists using bacterial growth methods, and DNA testing using Polymerase Chain Reaction (PCR) methods (*6*,*8*,*9*,*12*,*13*,*16*−*21*). Visual inspection is highly susceptible to human error, and HLB may be present for up to several years before visual symptoms are present (*9*). The bacterium associated with HLB does not grow well on plates used to detect most microbiological samples. PCR has, thus far, proven to be the best method available for HLB detection. However, it is also costly and time-consuming. Fourier transform infrared (FTIR) spectroscopy may be a useful method for early detection of HLB disease. FTIR spectrometers are available that are portable enough to be used in the field and can give results in minutes instead of hours. Additionally, FTIR-attenuated total reflection (ATR) spectroscopy requires very little sample and can be repeated many times very quickly to verify results. It has previously been shown to be effective in discriminating between leaves from apparently healthy citrus plants and those infected with HLB disease (*22*). The objective of the current study is to focus on the ability of the FTIR spectroscopic method to distinguish HLB-infected plants from other plants with various common citrus plant maladies.

*Author to whom correspondence should be addressed [e-mail Samantha.hawkins@ars.usda.gov; telephone (706) 546-3454; fax (706) 546-3607].

This article not subject to U.S. Copyright. Published XXXX by the American Chemical Society

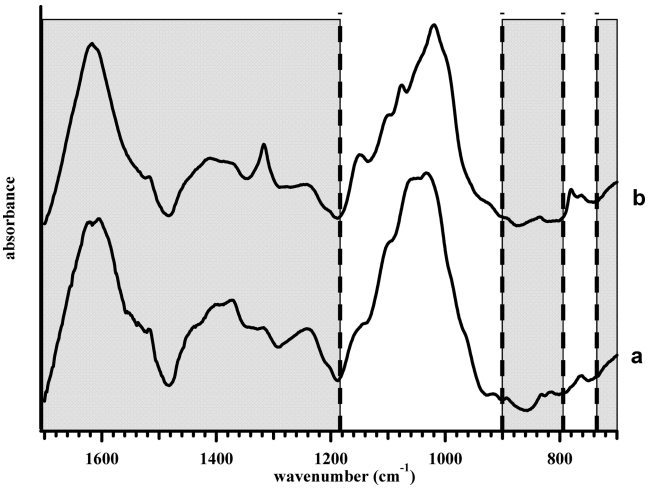

Figure 1. FTIR spectra of (a) disease-free and (b) HLB-positive samples of leaves collected from grapefruit trees. The regions from 735 to 795 cm^{-1} and from 900 to 1185 cm^{-1} were used to create a chemometric model, which may be used to predict the HLB status of citrus plants. (Spectra are offset for clarity.)

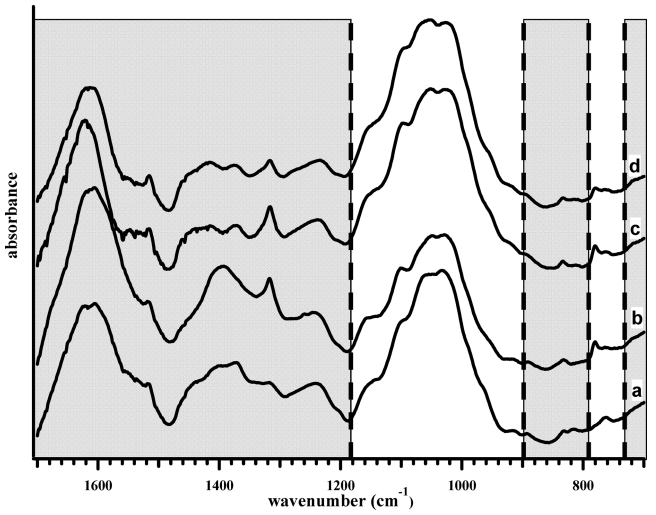

Figure 2. FTIR spectra (fingerprint region shown) of typical spectra from (a) apparently healthy citrus leaves, (b) leaves from citrus plant with Fe deficiency, (c) leaves from citrus plant with CPsV, and (d) leaves from citrus plant with CLRV. The plants from which these specific spectra were taken, except for the healthy sample, exhibited signs of chlorosis or dark veins. The chemometric model identified these as HLB negative. (Spectra are offset for clarity.)

MATERIALS AND METHODS

Samples of grapefruit leaves (Duncan and Ruby Red) grown under controlled conditions were collected from the USDA-ARS HRL greenhouses in Fort Pierce, FL. A total of 238 separate samples were collected for use in this study. Samples were obtained from plants that were exposed to individual citrus diseases or deficiencies. The diseased leaves came from plants that were inoculated with one of the following: CLRV, CTV, CPsV, canker, or HLB. To create plants with nutrient deficiency maladies, 28 plants were grown in 3.8 L containers in washed builder's sand. Nutrient solutions (treatments) were prepared according to the method described by Hoagland and Arnon (*23*), with iron being supplied as an EDTA acid. Treatments consisted of complete nutrition (i.e., containing all plant-essential nutrients) as a control and then five other treatments with each solution lacking one of the following minerals: copper, iron, magnesium, manganese, or zinc. There was an additional treatment that received no nutrients at all, just distilled−deionized water. Treatments (1000 mL) were applied weekly to each of the four replications of the seven treatments.

Several leaves were collected from each plant in the study and combined to test as a single sample. Some of the infected plants had leaves that were asymptomatic. Thus, some of the tested samples were from leaves that showed no outward signs of infection even though the entire plant was infected with a particular disease. The method of preparation for real-time PCR and FTIR analysis has been described in detail previously (*22*). Briefly, several leaves were selected from each plant and combined to form a single sample. The midrib vein of a leaf was separated from the rest of the leaf and combined with the other veins for a particular sample for testing by real-time PCR. The remainder of the leaves for that sample were dried in a 1250 W microwave oven for 3 min at half-power and ground into a powder in a Kleco 4200 Tissue Pulverizer (Garcia Manufacturing, Visalia, CA) for FTIR-ATR spectroscopy. For real-time PCR analysis, the DNA was isolated using a modified sodium dodecyl sulfate/potassium acetate extraction method (*24*). Analysis of 2 μL of sample was performed in duplicate via a 7500 Fast Real-time PCR system (Applied Biosystems, Foster City, CA) using Invitrogen Express Premix (Carlsbad, CA), along with primers and probe (labeled with NED-MGB) developed by Li (*25*). Real-time PCR analysis was used to obtain a critical threshold (C_t) value for each sample with regard to the presence of HLB disease. A value at or below 30 is considered to be positive, a value at or above 32 is considered to be negative, and between 30.01 and 31.99 is a "gray" area where the presence of the HLB disease is unclear (*22*).

The ATR spectra were collected using a Thermoelectron Nicolet (Madison, WI) Magna 850 FTIR spectrometer with a deuterated triglycine sulfate (DTGS) detector. A diamond crystal ATR (Durascope, Smiths Detection, Danbury, CT) accessory was used, and no further sample preparation was necessary. The spectra were acquired with 2 cm^{-1} resolution and a co-addition of 128 scans. The sample spectra were background subtracted using a spectrum collected in the absence of any sample.

A method for identifying the typical spectra of HLB-infected citrus plants has been reported in a recent study (*22*). The spectra of infected and healthy plants collected for the prior work were used to develop a chemometric model, which is used for the prediction of the presence of HLB in the plants in the current reported work. The spectra were analyzed using the Unscrambler (version 9.8 from Camo Software, Woodbridge, NJ) software. The region from 1765 to 4000 cm^{-1} was not included in the analysis due to interference from the diamond ATR crystal and remaining water in the samples. The spectra were baseline corrected with a scalar baseline offset and were normalized using area normalization. Subsets of the 700−1765 cm^{-1} region, specifically the areas between 735 and 795 cm^{-1} and between 900 and 1185 cm^{-1} of the spectra from 47 healthy plants and 110 HLB-infected plants of the mid-IR were used to create models for the prediction of the presence of HLB disease. A chemometric model was developed using principal component regression, which is a two-part method. Principal component analysis of the spectra is followed by multiple linear regression and features full cross-validation to reach an optimal model with which predictions can be made. The model developed was optimized with three principal components.

RESULTS AND DISCUSSION

Typical ATR spectra from disease-free citrus plants and HLB positive citrus plants are shown in **Figure 1**. The carbohydrate region of the spectrum, between 900 and 1185 cm^{-1}, is the region that has been shown to be the most significant in terms of identifying HLB disease (*22*). In healthy plants, the spectra have a carbohydrate region that has a broad flat peak centered around 1052 cm^{-1} and weak shoulders at 1077 and 1150 cm^{-1}. The HLB-infected plants have spectra with a large, sharp, asymmetrical peak at 1020 cm^{-1} and sharp peaks instead of weak shoulders at 1077 and 1150 cm^{-1}. Comparison of the FTIR spectrum of healthy citrus leaves to that of HLB-infected leaves reveals a clear difference in the carbohydrates that are present in each plant (see **Figure 1**). The specific carbohydrates that are present have not been identified here, but may be identified with other analytical chemistry techniques. In the current study, the FTIR spectra of some of the unhealthy plant leaves more closely resemble healthy

plants when FTIR spectra are examined, and some more closely resemble the HLB-infected plants.

The chemometric model was used to predict whether or not the HLB infection was present in the 238 plants in this study with the hopes that HLB could be uniquely identified by examining plants that might be infected with various citrus diseases. Both the 735−795 and 900−1185 cm^{-1} regions that were used to develop the model contain significant peaks that can be attributed to carbohydrate vibrational bands in the mid-IR spectrum (*26*). All manner of carbohydrates have peaks in these regions including, but not limited to, starches, cellulose, sugars, and polysaccharides (*26*−*29*). The model developed using the healthy and HLB-infected citrus leaves was used to predict the C_t values (with respect to HLB PCR evaluation). In the current study there were 20 samples that were presumptively identified as having a HLB infection via visual symptoms. Of those samples, only 17 were identified as having HLB (C_t below 30) by real-time PCR testing. Of the other 218 samples that were collected for this study (i.e., CLRV, CTV, CPsV, canker, nutrient deficiencies, and control samples), all were found to have C_t values above 32, indicating the absence of the HLB disease.

The model was completely accurate in excluding HLB disease as the culprit with only three of the citrus maladies represented in this study. The three types were 17 samples of plants infected with CLRV, 10 infected with CPsV, and 20 that were iron deficient. Typical spectra of these three types are shown in **Figure 2**. Some of the plants affected by these maladies exhibit symptoms including chlorosis, blotches, and dark veins. As shown in **Figure 2**, plants that exhibit disease symptoms can be accurately predicted to be free of HLB disease by chemometric analysis of the FTIR spectra.

With the other nutrient-deficient and virally infected samples, there were various degrees of accuracy in excluding or including HLB disease as the source of the plants' disease. The plants that were all nutrient deficient had spectra nearly identical to those of the HLB-infected plants that were used to create the model. Nineteen of 20 samples collected from all of the nutrient-starved plants were predicted to be HLB positive (see **Figure 3**). The next group with the spectra most similar to those of the HLB plants was the manganese-deficient plants, which had 16 of 20 predicted as HLB positive (see **Figure 3**). Citrus canker infected plants were predicted to be HLB positive in 14 of 19 samples (see **Figure 3**). Copper and zinc deficiencies also had a high degree of similarity in their spectra with 10 of 20 and 12 of 20, respectively, predicted as HLB positive (see **Figure 4**). One other set of samples with a citrus disease, CTV, also had a significant number of samples (12 of 39) that were predicted as HLB positive (see **Figure 5**). Samples from plants that were deficient in magnesium had 4 of 18 samples that were predicted to be HLB positive (spectra not shown). There were 32 samples, from a combination of the diseases, that were predicted in the "gray area" with C_t values between 30 and 32 that cannot be accurately described as positive or negative predictions.

The leaves used in this study varied in the visual symptoms of the various diseases with which they were infected. Many had no symptoms present at the time of collection, whereas others had full-blown visual symptoms. Various stages were used as a means to test the efficacy of the model for both prediction of the presence of disease and identifying HLB versus another disease. The FTIR spectra of the samples that were predicted as HLB positive all indicate that the leaves have a different carbohydrate present than that present in healthy plants. HLB disease interferes with the plant's phloem and its ability to carry nutrients throughout the plant (*30*). This could possibly be why there is a striking similarity of the spectra of plants with HLB disease and those that are nutrient deficient. In this study the plants infected with the HLB disease were provided fertilizer containing all nutrients. However, HLB blocks the plants' ability to fully utilize the available nutrients. Many of the infected plants show signs of change in

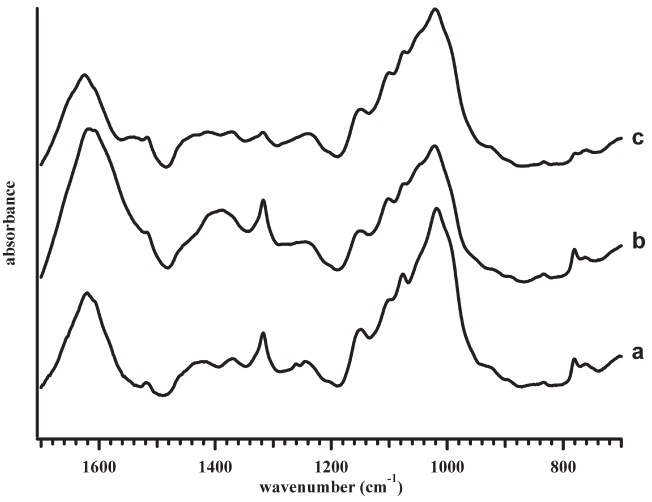

Figure 3. Typical FTIR spectra of leaves from (a) citrus plants that were deprived of all nutrients, (b) citrus plants deprived of manganese, and (c) citrus plants infected with citrus canker. (Spectra are offset for clarity.)

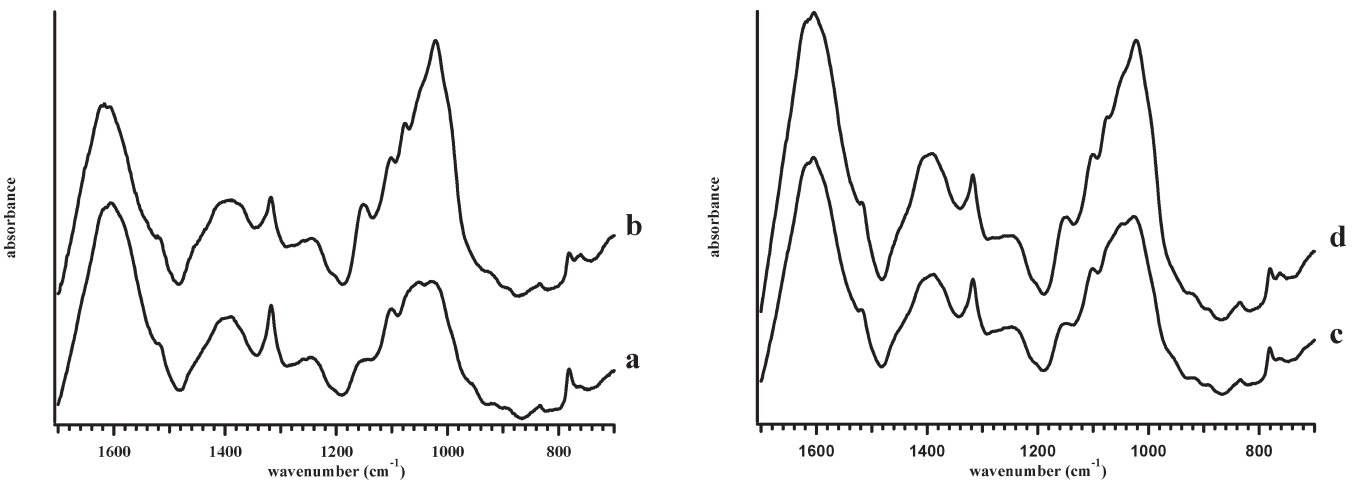

Figure 4. FTIR spectra of leaves from (a) a copper-deficient citrus plant that was predicted to be HLB negative, (b) a copper-deficient citrus plant predicted to be HLB positive, (c) a zinc-deficient citrus plant predicted to be HLB negative. and (d) a zinc-deficient citrus plant predicted to be HLB positive. All of these plants were in fact HLB negative, as tested by PCR experiments. (Spectra are offset for clarity.)

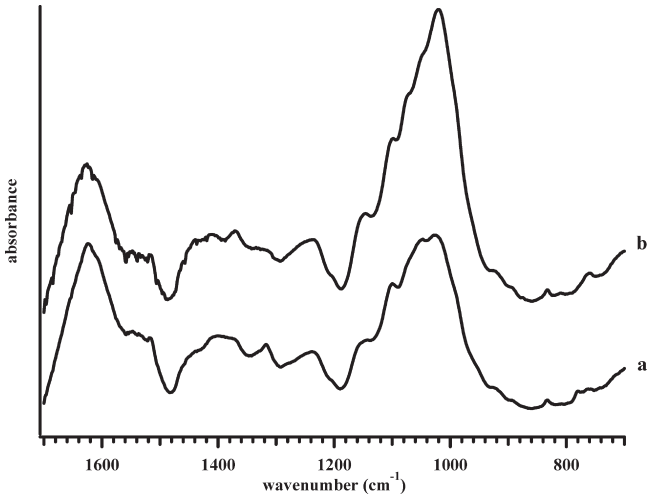

Figure 5. FTIR spectra from citrus plants infected with Citrus tristeza virus (HLB negative as shown with PCR testing): (a) predicted to be HLB negative by the chemometric model; (b) predicted to be HLB positive by chemometric model. (Spectra are offset for clarity.)

the FTIR spectra before the plants have begun to display visual symptoms as indicated in the figures. The ability of FTIR spectroscopy to show the changes in the chemistry of the plant before visible symptoms in many of the samples, along with its ease of use, speed, and relative cost, could lead to its increased use as a predictive method in the future.

LITERATURE CITED

(1) Roy, A.; Fayad, A.; Barthe, G.; Brlansky, R. H. A multiplex polymerase chain reaction method for reliable, sensitive and simultaneous detection of multiple viruses in citrus trees. *J. Virol. Methods* **2005**, *129*, 47–55.

(2) Gonsalves, D.; Purcifull, D. E.; Garnsey, S. M. Purification and serology of citrus tristeza virus. *Phytopathology* **1978**, *68*, 553–559.

(3) Qin, J.; Burks, T. F.; Ritenour, M. A.; Bonn, W. G. Detection of citrus canker using hyperspectral reflectance imaging with spectral information divergence. *J. Food Eng.* **2009**, *93*, 183–191.

(4) www.sepdn.org.

(5) www.clemson.edu/public/regulatory/plant_prob_clinic/citrus_greening.pdf.

(6) Li, W.; Hartung, J. S.; Levy, L. Quantitative real-time PCR for detection and identification of *Candidatus Leberibacter* species associated with citrus huanglongbing. *J. Microbiol. Methods* **2006**, *66*, 104–115.

(7) Mishra, A.; Ehsani, R.; Albrigo, G.; Lee, W. S. *Spectral Characteristics of Citrus Greening* (*Huanglongbing*); ASABE Paper 073056; American Society of Agricultural and Biological Engineers: St. Joseph, MI, 2007.

(8) Manjunath, K. L.; Halbert, S. E.; Ramadugu, C.; Webb, S.; Lee, R. F. Detection of '*Candidatus* Liberibacter asiaticus' in *Diaphorina citri* and its importance in the management of citrus huanglongbing in Florida. *Phytopathology* **2008**, *98*, 387–396.

(9) Gottwald, T. R.; da Graca, J. V.; Bassanezi, R. B. Citrus huanglongbing: the pathogen and its impact. *Plant Health Prog.* **2007**, doi: 10.1094/PHP-2007-0906-01-RV.

(10) Srivastava, A. K.; Singh, S. Diagnosis of nutrient constraints in citrus orchards of humid tropical India. *J. Plant Nutr.* **2006**, *29*, 1061–1076.

(11) Srivastava, A. K.; Singh, S. Zinc nutrition, a global concern for sustainable citrus production. *J. Sustainable Agric.* **2005**, *25*, 5–42.

(12) Halbert, S. E.; Manjunath, K. L. Asian citrus psyllids (Strenorrhyncha: Psyllidae) and greening disease of citrus: a literature review and assessment of risk in Florida. *Fla. Entomol.* **2004**, *87*, 330–352.

(13) Bové, J. M. Huanglongbing, a destructive, newly-emerging, century-old disease of citrus. *J. Plant Pathol.* **2006**, *88*, 7–37.

(14) www.doacs.state.fl.us/pi/chrp/greening/StatewidePositiveHLBSections.pdf.

(15) www.aphis.usda.gov/plant_health/plant_pest_info/citrus_greening.

(16) Cubero, J.; Graham, J. H.; Gottwald, T. R. Quantitative PCR method for diagnosis of citrus bacterial canker. *Appl. Environ. Microbiol.* **2001**, *67*, 2849–2852.

(17) do Carmo Teixeira, D.; Saillard, C.; Eveillard, S.; Danet, J. L.; da Costa, P. I.; Ayres, A. J.; Bové, J. '*Candidatus* Liberibacter americanus', associated with citrus huanglongbing (greening disease) in São Paulo State, Brazil. *Int. J. Systematic Evol. Microbiol.* **2005**, *55*, 1857–1862.

(18) do Carmo Teixeira, D.; Danet, J. L.; Eveillard, S.; Martins, E. C.; de Jesus Junior, W. C.; Yamamoto, P. T.; Lopes, S. A.; Bassanezi, R. B.; Ayres, A. J.; Saillard, C.; Bové, J. M. Citrus huanglongbing in São Paulo State, Brazil: PCR detection of the '*Candidatus*' Liberibacter species associated with the disease. *Mol. Cell. Probes* **2005**, *19*, 173–179.

(19) Lin, H.; Doddapaneni, H.; Bai, X.; Yao, J.; Zhao, X.; Civerolo, E. L. Acquisition of uncharacterized sequences from *Candidatus* Liberibacter, an unculturable bacterium, using an improved genomic walking method. *Mol. Cell. Probes* **2008**, *22*, 30–37.

(20) Qin, J.; Burks, T. F.; Kim, M. S.; Chao, K.; Ritenour, M. A. Detecting citrus canker by hyperspectral reflectance imaging and PCA-based image classification method. *Proc. SPIE* **2008**, *6983*, 698305.

(21) Qin, J.; Burks, T. F.; Kim, D. G.; Bulanon, D. M. *Classification of Citrus Peel Diseases Using Color Texture Feature Analysis*; ASABE Food Processing Automation Conference Paper 701P0508cd; American Society of Agricultural and Biological Engineers: St. Joseph, MI, 2008.

(22) Hawkins, S.; Park, B.; Poole, G.; Gottwald, T.; Windham, W.; Lawrence, K. Detection of citrus huanglongbing by FTIR-ATR spectroscopy. *Appl. Spectrosc.* **2010**, *64*, 100–103.

(23) Hoagland, D. R.; Arnon, D. I. The water culture method for growing plants without soil *Calif. Agric. Expt. Stn. Circ. 347*, 1950.

(24) De Paulo, J. J.; Powell, C. A. Extraction of double-stranded RNA from plant tissues without the use of organic solvents. *Plant Dis.* **1995**, *79*, 246–248.

(25) Li, W.; Hartung, J; Levy, L. Quantitative real-time PCR for detection and identification of *Candidatus* Liberibacter species associated with citrus huanglongbing. *J. Microbiol. Methods* **2006**, *66*, 104–115.

(26) Lammers, K.; Arbuckle-Keil, G.; Dighton, J. FT-IR study of the changes in carbohydrate chemistry of three New Jersey pine barrens leaf litters during simulated control burning. *Soil Biol. Biochem.* **2009**, *41*, 340–347.

(27) Khurana, H. K.; Jun, S.; Cho, I. K.; Li, Q. X. Rapid determination of sugars in commercial fruit yogurts and yogurt drinks using Fourier transform infrared spectroscopy and multivariate analysis. *Appl. Eng. Agric.* **2008**, *24*, 631–636.

(28) van Soest, J. J. G.; Tournois, H.; de Wit, D.; Vliegenthart, J. F. G. Short-range structure in (partially) crystalline potato starch determined with attenuated total reflectance Fourier-transform IR spectroscopy. *Carbohydr. Res.* **1995**, *279*, 201–214.

(29) Vasko, P. D.; Blackwell, J.; Koenig, J. L. Infrared and Raman spectroscopy of carbohydrates: Part I. Identification of O—H and C—H related vibrational modes for D-glucose, maltose, cellobiose, and dextran by deuterium-substitution methods. *Carbohydr. Res.* **1971**, *19*, 297–310.

(30) Kim, J.; Sagaram, U. S.; Burns, J. K.; Li, J.; Wang, N. Response of sweet orange (*Citrus sinensis*) to 'Candidatus Liberibacter asiaticus' infection: microscopy and microarray analyses. *Phytopathology* **2009**, 50–57.

Received for review December 2, 2009. Revised manuscript received April 16, 2010. Accepted April 26, 2010.